Synthesis and Characterization of a New Series of Nickel(II) *meso*-Tetrakis (polyfluorophenyl)porphyrins Functionalized by Pyrrole Groups and Their Electropolymerized Films

Maria A. Carvalho de Medeiros, Serge Cosnier,* Alain Deronzier,* and Jean-Claude Moutet

Laboratoire d'Electrochimie Organique et de Photochimie Rédox (URA CNRS 1210), Université Joseph Fourier Grenoble 1, BP 53, 38041 Grenoble Cedex 9, France

Received August 4, 1995[⊗]

A new series of nickel(II) *meso*-tetrakis(polyfluorophenyl)porphyrins functionalized by pyrrole groups have been synthesized. Each new complex was isolated and characterized by ^{1}H NMR, ^{19}F NMR, IR, UV−visible spectroscopy, and mass spectrometry as well as electrochemistry. This is the first example of polyfluorinated substituted porphyrins where the four possible compounds have been obtained by functionalization of the *para*-fluorine substituents of the nickel(II) *meso*-tetrakis(pentafluorophenyl)porphyrin. This functionalization has allowed the preparation for the first time of polyfluorinated metalloporphyrin films by oxidative electropolymerization. Electrochemical stability studies of these polymeric films have shown better stability for films derived from the monomer having four pyrrole groups because of their high degree of cross-linking degree. A large difference of electroactive solute permeation has been found in the polymeric films which have been obtained by electropolymerization of monomers for which one pyrrole group has been substituted compared to those for which four pyrrole groups have been substituted. This could be related to quite rigid polymer structures for tetrasubstituted polymer films and molecular sieving properties of monosubstituted polymer films. The spectroelectrochemistry of a polymeric film on an OTE has established that the two-electron-oxidized species are stable in the film; likewise the singly and doubly electroreduced species are stable and are more likely ligand-centered.

Introduction

Numerous studies on metalloporphyrin catalysis have demonstrated that polyhalogenated metalloporphyrins are robust catalysts for alkane hydroxylation and olefin epoxidation.[1−5] The catalyst stability, in particular, is markedly enhanced via substitution of the metalloporphyrin macrocycle by electron-withdrawing pentafluorophenyl groups.[2−8] Current interest is also in supported metalloporphyrins which is directed toward developing oxidation catalysts that combine the versatility of homogeneous metalloporphyrins [2] with the advantages of heterogeneous systems. In this connection, production and application of modified electrodes by films of polymers containing metalloporphyrins have been developed.[9,10] For instance, we recently reported the application to electrocatalytic biomimetic oxidation of drugs of a series of poly(pyrrole−manganese tetraphenylporphyrin)-modified electrodes.[11] In that context, it would be useful to elaborate modified electrodes containing polyhalogenated metalloporphyrins. Thus we describe herein the synthesis and properties of a new series of nickel(II) *meso*-tetrakis(polyfluorophenyl) porphyrins functionalized by pyrrole-containing groups (R_1) (Figure 1) and their electropolymerized

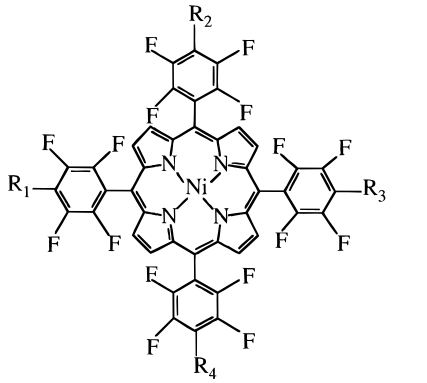

1a: R_1 = —O—$(CH_2)_3$—N, $R_2 = R_3 = R_4 = F$

1b: $R_1 = R_2$ = —O—$(CH_2)_3$—N, $R_3 = R_4 = F$

1c: $R_1 = R_2 = R_3$ = —O—$(CH_2)_3$—N, $R_4 = F$

1d: $R_1 = R_2 = R_3 = R_4$ = —O—$(CH_2)_3$—N

Figure 1. Structures of the **1a**−**d** compounds.

[⊗] Abstract published in *Advance ACS Abstracts,* April 1, 1996.

(1) Traylor, P. S.; Dolphin, D.; Traylor, T. G. *J. Chem. Soc., Chem. Commun*. **1984**, 279.
(2) Recent reviews on metalloporphyrins catalysis: (a) Meunier, B. *Chem. Rev*. **1992**, *92*, 1411. (b) Mansuy, D. *Coord. Chem. Rev*. **1993**, *125*, 129.
(3) Castellino, A. J.; Bruice, T. C. *J. Am. Chem. Soc*. **1988**, *110*, 158.
(4) Nappa, M. J.; Tolman, C. A. *Inorg. Chem*. **1985**, *24*, 4711.
(5) Battioni, P.; Renaud, J. P.; Bartoli, J. F.; Reina-Artiles, M.; Fort, M.; Mansuy, D. *J. Am. Chem. Soc*. **1988**, *110*, 8462.
(6) Chang, C. K.; Ebina, F. *J. Chem. Soc., Chem. Commun*. **1981**, 778.
(7) Traylor, T. G.; Kim, C.; Richards, J. L.; Xu, F.; Perrin, C. L. *J. Am. Chem. Soc*. **1995**, *117*, 3468 and references cited therein.
(8) Komuro, M.; Nagatsu, Y.; Higuchi, T.; Hirobe, M. *Tetrahedron Lett*. **1992**, *33*, 4949.
(9) Bedioui, F.; Devynck, J.; Bied-Charreton, C. *Acc. Chem. Res*. **1995**, *28*, 30.
(10) Deronzier, A.; Moutet, J.-C. *Acc. Chem. Res.* **1989**, *22*, 249; *Coord. Chem. Rev*. in press.
(11) Cauquis, G.; Cosnier, S.; Deronzier, A.; Galland, B.; Limosin, D.; Moutet, J.-C.; Bizot, J.; Deprez, D.; Pulicani, J.-P. *J. Electroanal. Chem. Interfacial Electrochem*. **1993**, *352*, 181.

0020-1669/96/1335-2659$12.00/0

films. By extending a synthetic procedure previously reported by Traylor et al.[12] for polyfluorinated porphyrins (or their Zn (II) and Fe (III) complexes), we were able to synthesize and for the first time separate and characterize the four possible compounds obtained by functionalization of the *para*-fluorine atoms of nickel(II) *meso*-tetrakis(pentafluorophenyl)porphyrin. Here a pyrrole alcoholate was used as nucleophile. As will be demonstrated in this paper, the polymeric films obtained from the electropolymerization of **1a**−**d** monomers have different electrochemical properties and exhibit large differences in permeation according to their degree of cross-linking.

Experimental Section

Materials. The following solvents and common laboratory chemicals employed in the preparation of the compounds were reagent grade and were used without further purification: deuterated chloroform ($CDCl_3$, Aldrich), dichloromethane (HPLC grade, SDS), tetrachloro-1,4-benzoquinone (*p*-chloranil, Aldrich), 2,3-dichloro-5,6-dicyano-1,4-benzoquinone (DDQ, Aldrich), pentafluorobenzaldehyde (Janssen Chimica), boron trifluoride etherate ($BF_3{\cdot}Et_2O$, Aldrich), nickel(II) acetate tetrahydrate ($Ni(C_2H_3O_2)_2{\cdot}4H_2O$, Janssen Chimica), 3-amino-1-propanol (Janssen Chimica), 2,5-dimethoxytetrahydrofuran (Janssen Chimica). Tetrahydrofuran (THF) was purchased from SDS and distilled from lithium aluminum hydride (Fluka). Cyclohexane was obtained from Janssen Chimica and distilled before use. Pyrrole (Aldrich) was distilled at atmospheric pressure before use. The porphyrins were chromatographed on a silica gel column (70−230 mesh, Matrex).

Physical Measurements. NMR spectra were obtained on a Bruker AC 200 MHz FT-NMR spectrometer using $CDCl_3$ as solvent. ^1H and ^{19}F NMR spectra were quoted as δ (ppm) vs tetramethylsilane (TMS) and $CFCl_3$, respectively.

UV−visible spectra were collected by use of a Cary 1 UV−vis spectrophotometer interfaced with an Epson Ax 2e PC computer. The measurements were made in standard 1 mm quartz cuvettes.

Infrared (IR) spectra were recorded by use of a Nicolet Impact 400 FT-IR spectrophotometer interfaced with a PC computer. IR measurements were made either in KBr pellets or in a demountable cell with KBr plates.

Fast atom bombardment (FAB) mass spectra were obtained on a AIE Kratos MS 50 mass spectrometer fitted with an Ion Tech Ltd. gun at the mass spectrometry service UJF-CNRS, CERMAV, Grenoble, France. A standard FAB source was used, and *m*-nitrobenzyl alcohol (NBA) was the liquid matrix.

Elemental analyses were performed by Service Central d'Analyses−CNRS, Vernaison, France.

Synthesis and Purification. (a) 5,10,15,20-Tetrakis(pentafluorophenyl)porphyrin (H_2F_{20}TPP) was synthesized via the condensation of pyrrole and pentafluorobenzaldehyde according to the method reported by Lindsey[13,14] using either DDQ or *p*-chloranil (3 equiv (per porphyrinogen)) as the oxidant. The yield obtained was ca. 30%, which agreed with that published recently[15] with 1 mM $BF_3{\cdot}Et_2O$ as catalyst. H_2F_{20}TPP was characterized by ^1H and ^{19}F NMR spectroscopy (Table 1).

(b) NiF_{20}TPP. The nickel(II) complex of H_2F_{20}TPP was prepared using the method reported by Kadish[16] and was characterized by ^1H and ^{19}F NMR spectroscopy (Table 1).

Mass spectral data ($C_{44}H_8F_{20}N_4Ni$): calculated MW 1031.23; *m/e* of parent peak at 1030. UV−visible data [λ_{max}, nm ($10^{-4}\epsilon$, M^{-1} cm^{-1})], CH_3CN: 399 (20.1), 521(1.44), 555 (1.23). IR (KBr): 1064, 1080 cm^{-1}.

Table 1. ^1H and ^{19}F NMR Data Recorded in $CDCl_3$[a]

compound	^1H NMR							^{19}F NMR[b]				
	NH	OH	CH_2	CH_2O	CH_2N	H-3,4	H-2,5	pyrrole β	*o*-F′	*o*-F″	*p*-F	*m*-F″	*m*-F″
H_2F_{20}TPP	−2.92 (s)							8.92 (s)	−136.95 (m)		−151.67 (t)		−161.77 (m)
NiF_{20}TPP								8.79 (s)	−137.70 (m)		−151.67 (t)		−161.77 (m)
1-(3-hydroxypropyl)pyrrole		2.04 (m)	1.94 (m)	3.58 (t)	4.00 (m)	6.15 (t)	6.65 (m)						
monomer **1a**			2.40 (m)	4.30 (t)	4.46 (t)	6.24 (t)	6.80 (t)	8.84 (m)	−137.08 (m)	−138.96 (m)	−151.85 (t)	−157.12 (m)	−161.68 (m)
monomer **1b**			2.39 (m)	4.30 (t)	4.45 (t)	6.23 (t)	6.79 (t)	8.78 (m)	−137.07 (m)	−138.94 (m)	−151.96 (t)	−157.17 (m)	−161.75 (m)
monomer **1c**			2.41 (m)	4.30 (t)	4.45 (t)	6.24 (t)	6.80 (t)	8.79 (m)	−137.05 (m)	−138.92 (m)	−152.06 (t)	−157.21 (m)	−161.80 (m)
monomer **1d**			2.38 (m)	4.31 (m)	4.45 (t)	6.24 (t)	6.80 (t)	8.80 (m)		−138.91 (m)		−157.25 (m)	

[a] In ppm; ^1H NMR vs TMS; ^{19}F NMR vs $CFCl_3$; s = singlet; t = triplet; m = multiplet. [b] F′ are in unsubstituted pentafluorophenyl groups, and F″ are in substituted pentafluorophenyl groups.

(12) Battioni, P.; Brigaud, O.; Desvaux, H.; Mansuy, D.; Traylor, T. G. *Tetrahedron Lett.* **1991**, *32*, 2893.
(13) Lindsey, J. S.; Schreiman, I. C.; Hsu, H. C.; Kearney, P. C.; Marguerettaz, A. M. *J. Org. Chem.* **1987**, *52*, 827.
(14) Lindsey, J. S.; Wagner, R. W. *J. Org. Chem.* **1989**, *54*, 828.
(15) La, T.; Richards, R.; Miskelly, G. M. *Inorg. Chem.* **1994**, *33*, 3159.
(16) Kadish, K. M.; Aroullo-McAdams, C.; Han, B. C.; Franzen, M. M. *J. Am. Chem. Soc.* **1990**, *112*, 8364.

(c) 1-(3-Hydroxypropyl)pyrrole. This compound was prepared as described previously[17] and was characterized by ^{1}H NMR spectroscopy (Table 1).

(d) 1a−d Monomers. The synthesis of the **1a−d** monomers which contain one, two, three, and four 3-(pyrrol-1-yl)propyloxy groups (R_1), respectively, covalently linked to the macrocycle by the substitution of the *para*-F atoms of $NiF_{20}TPP$ was accomplished by the following procedure: initially 1-(3-hydroxypropyl)pyrrole (1.7×10^{-3} mol) was refluxed in THF (10 mL) with Na (1.7×10^{-2} mol) for 6 h in a drybox (Ar atmosphere). The solution was cooled to ca. 20 °C, and then 2 equiv of this solution (3.8×10^{-4} M) was reacted with 1 equiv of $NiF_{20}TPP$ (1.9×10^{-4} mol) in refluxing THF (10 mL) overnight in a drybox (Ar atmosphere). The solvent was evaporated, and then the product was washed with H_2O and extracted with CH_2Cl_2. The extract was dried over anhydrous Na_2SO_4 and filtered, and the solvent was removed via rotary evaporation. The crude product was then chromatographed by using a silica gel column with a 1:1 cyclohexane/CH_2Cl_2 mixture as eluting solvent. The first of the five major bands which eluted was red-purple and was identified as unreacted NiF_{20}-TPP. The other bands were also red-purple. The second band was collected, and after a second chromatographic procedure using a silica gel column with a 1:1 cyclohexane/CH_2Cl_2 mixture as eluting solvent, the product obtained, after solvent evaporation, was identified as the **1a** compound corresponding to the monosubstitution of a *para*-F atom of $NiF_{20}TPP$ by a 3-(pyrrol-1-yl)propyloxy group (R_1) (ca. 20% yield).

1a Monomer. UV−visible data [λ_{max}, nm (ϵ x 10^{-4}, M^{-1} cm^{-1})], CH_3CN: 400 (19.7), 521 (1.4), 555 (1.21). Mass spectral data ($C_{51}H_{18}F_{19}N_5ONi$): calculated MW 1136.39; *m/e* of parent peak at 1136. IR (KBr): 1064, 1084, 1283 cm^{-1}.

The third major band was collected, and after a purification procedure similar to that for the second band, the product obtained was identified as the **1b** compound with disubstitution of the *para*-F atoms by pyrrole-containing groups (R_1) (ca. 10% yield). It should noted that this band probably corresponds to a mixture of the two possible isomers (see Figure 1).

1b Monomer. UV−visible data [λ_{max}, nm (ϵ x 10^{-4}, M^{-1} cm^{-1})], CH_3CN: 400 (19.1), 521 (1.37), 555 (1.17). Mass spectral data ($C_{58}H_{28}F_{18}N_6O_2Ni$): calculated MW 1241.56; *m/e* of parent peak 1242. IR (KBr): 1067, 1084, 1283 cm^{-1}.

The fourth band was collected, and after a purification procedure similar to that used for the second band, the product obtained was identified as the **1c** compound with trisubstitution of the *para*-F atoms by pyrrole-containing groups (R_1) (ca. 17% yield).

1c Monomer. UV−visible data [λ_{max}, nm (ϵ x 10^{-4}, M^{-1} cm^{-1})], CH_3CN: 400 (18.7), 521 (1.34), 555 (1.14). Mass spectral data ($C_{65}H_{38}F_{17}N_7O_3Ni$): calculated MW 1346.73; *m/e* of parent peak 1346. IR (KBr): 1069, 1086, 1283 cm^{-1}.

Finally, the fifth band was collected, and after a purification procedure similar to that for the second band, the product obtained was identified as the **1d** compound with tetrasubstitution of the *p*ara-F atoms by pyrrole-containing groups (R_1) (ca. 25% yield).

1d Monomer. UV−visible data [λ_{max}, nm (ϵ x 10^{-4}, M^{-1} cm^{-1})], CH_3CN: 401 (18.3), 521 (1.3), 555 (0.98). Mass spectral data ($C_{72}H_{48}F_{16}N_8O_4Ni$): calculated MW 1451.88; *m/e* of parent peak 1452. Anal. Calcd for **1d**: C, 60.25; H, 3.64; F, 19.35. Found: C, 59.91; H, 3.57; F, 19.36. IR (KBr): 1069, 1086, 1283 cm^{-1}.

Electrochemistry. All electrochemical experiments were performed with a Princeton Applied Research Model 173 potentiostat equipped with a Model 179 digital coulometer and a Model 175 universal programmer. A Sefram TGM 164 X-Y recorder was used for plotting cyclic voltammograms. All experiments were run at room temperature in a drybox under an argon atmosphere with a normal three-electrode configuration. Acetonitrile (Rathburn, HPLC grade) was used as received. Tetrabutylammonium perchlorate (TBAP) (Fluka puriss) was recrystallized from ethyl acetate/cyclohexane and vacuum-dried at 80 °C 3 days before use. The working electrode was a glassy carbon disk (diameter 5 mm) polished with 1 μm diamond paste. All potentials were referred to the Ag/Ag^+ (10 mM in CH_3CN + 0.1 M TBAP) reference electrode. The counter electrode was platinum gauze. Typical nickel(II) porphyrin concentrations for cyclic voltammetry were in the range 10^{-3}−10^{-4} M.

Apparent surface coverages of immobilized species (Γ) were determined from the charge under the two-electron-oxidation peaks of the metalloporphyrin.

Spectroelectrochemistry. UV−visible spectroelectrochemistry measurements on films were made using a conventional sandwich-type cell[18] in a drybox under an argon atmosphere. Spectral changes were monitored by a Hewlett-Packard HP 8452A diode array spectrophotometer interfaced with a Compaq 286 computer. The optically transparent conductive electrode (OTE) (diameter 1.1 cm) was doped with indium tin oxide (ITO) (Balthracon Z20 from Balzers).

Results and Discussion

Synthesis and Characterization. *meso*-Tetrakis(pentafluorophenyl)porphyrin was synthesized using the methodology reported by Lindsey[13,14] with yield and purity in accordance with recent results.[15] This approach gives a better yield than that reported by Longo.[19] The regiospecific substitution of fluorine by pyrrole-containing groups (R_1) was accomplished, and confirmed by ^{1}H and ^{19}F NMR, IR, mass spectra, electrochemistry, and elemental analysis. These data showed consistency with the calculated molecular weights for all assigned structures of the **1a−d** compounds (Figure 1). ^{1}H and ^{19}F NMR spectral data for this new series of nickel(II) porphyrins are summarized in Table 1. It should be noted that all proton NMR spectra show integration ratios consistent with these assigned structures. The results reveal that the reaction of a pyrrole alcoholate group (R_1) with $NiF_{20}TPP$ occurs by a substitution of the most reactive F atom (*para*-position) of an electron-withdrawing pentafluorophenyl group in accordance with that published previously for other nucleophiles.[12] ^{19}F NMR spectra of all complexes are shown in Figure 2. The *ortho*-fluorine atoms are the most downfield and appear at ca. −137 ppm for an *ortho*-F in an unsubstituted pentafluorophenyl group and at ca. −139 ppm for an *ortho*-F in an aryl group substituted by a pyrrole-containing group (R_1). The resonance recorded at ca. −152 ppm (triplet signal) is attributed to the *para*-F of each group. The resonances for the *meta*-F atoms are the most upfield and appear at ca. −162 ppm for *meta*-F atoms in the unsubstituted aryl group and at ca. −157 ppm for those in a substituted aryl group (see Table 1). The relative intensities of integration of these signals are in agreement with the structures attributed to **1a−d.** The monosubstituted **1a** compound (Figure 2B) gives a ratio of 6:2:3:2:6 for *ortho*-F in the unsubstituted aryl groups, *ortho*-F in the substituted aryl group, *para*-F in the unsubstituted aryl groups, *meta*-F in the substituted aryl group, and *meta*-F in the unsubstituted aryl groups, respectively, and likewise 4:4:2:4:4 (Figure 2C) for the **1b** disubstituted and 2:6:1:6:2 (Figure 2D) for the **1c** trisubstituted compound. The tetrasubstituted **1d** compound appears at lower fields than that recorded for $NiF_{20}TPP$ (Figure 2A). Similar phenomena were previously published by Kadish[16] for other electron-donating substituents.

Redox Behavior of Monomers 1a−d. The cyclic voltammograms of $NiF_{20}TPP$, **1a** and **1d** monomers recorded in CH_3CN + 0.1 M TBAP, are shown in Figure 3 and a summary of reduction and oxidation potentials of the **1a−d** complexes is given in Table 2. Upon reductive scanning, the voltammograms

(17) Carpio, H.; Galeazzi, E.; Greenhouse, R.; Guzman, A.; Velarde, E.; Antonio, Y.; Franco, F.; Leon, A.; Perez, V.; Salas, R.; Valdes, D.; Ackrell, J.; Cho, D.; Gallegra, P.; Halpern, O.; Koehler, R.; Maddox, M. L.; Muchouwski, J. M.; Prince, A.; Tegg, D.; Thurber, T. C.; Van Horn, A. R.; Wren, D. *Can. J. Chem.* **1982**, *60*, 2295.

(18) Cosnier, S.; Deronzier, A.; Moutet, J.-C. *J. Phys. Chem.* **1985**, *89*, 4895.

(19) Longo, F. R.; Finarelli, M. G.; Kim, J. B. *J. Heterocycl. Chem.* **1969**, *6*, 927.

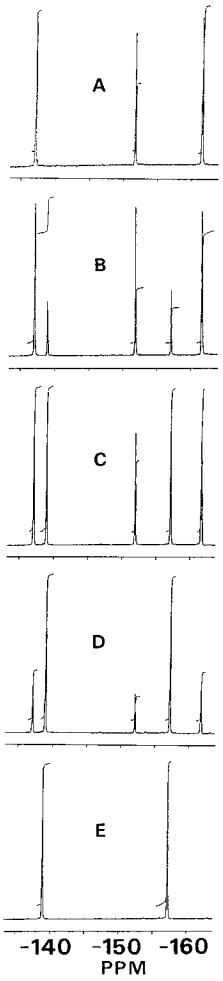

Figure 2. ^{19}F NMR spectra of (A) NiTFPP, (B) **1a** monomer, (C) **1b** monomer, (D) **1c** monomer, and (E) **1d** monomer in $CDCl_3$ (δ (ppm) vs $CFCl_3$).

show two reversible one-electron-peak systems for all complexes. It should be noted that the difference between the first and second reduction potentials is constant ($\Delta E_{1/2}$ = 0.54 V) whatever the complexes and may be compared to the 0.44 ± 0.04 V separation observed for the reduction at the π-ring system of porphyrin complexes yielding π-anion radicals ($P^{0/\bullet -}$) and dianions ($P^{\bullet -/2-}$).[20] Thus, as previously described for other nickel(II) porphyrins, these reductions could be assigned at ambient temperature to the reduction of the porphyrin ring, rather than reduction to Ni(I).[15,21−23] Upon oxidative scanning, the voltammogram for $NiF_{20}TPP$ (Figure 3A) exhibits a reversible two-electron-peak system, as established by the ratio of the peak intensities due to the metalloporphyrin oxidation and to the one-electron reduction of the metalloporphyrin (i^1_{pa}/i^2_{pc} = 2.02). This oxidation corresponds probably to the oxidation of the porphyrin ring (π-cation radical and dication) as reported previously for oxidation of (*para*-Cl) TPPNi in CH_2Cl_2 + 0.1 M TBAP[24] at ambient temperature, rather than oxidation to Ni-(III). It should be noted that, as expected, the replacement of highly-electron-withdrawing *para*-F atoms by a propyl ether

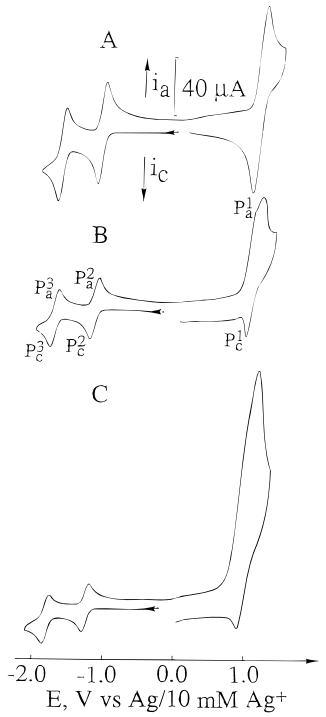

Figure 3. Cyclic voltammograms recorded at a glassy carbon electrode (diameter 5 mm) of (A) NiTFPP, (B) **1a** monomer, and (C) **1d** monomer in CH_3CN + 0.1 M TBAP. Scan rate = 0.1 V s^{-1}.

Table 2. Half-Wave Potentials ($E_{1/2}$) for the **1a**−**d** Complexes in CH_3CN with 0.1 M TBAP (Scan Rate = 0.1 V s^{-1})

	$E_{1/2}$[a], V (vs Ag/10 mM Ag^+)			
complex	redn 2	redn 1	oxidn[c]	$\Delta E_{1/2}^{red}$,[b] V
$NiF_{20}TPP$	−1.72	−1.18	1.03	0.54
monomer **1a**	−1.74	−1.20	1.02	0.54
monomer **1b**	−1.76	−1.22	1.01	0.54
monomer **1c**	−1.78	−1.24	1.00	0.54
monomer **1d**	−1.80	−1.26	0.99	0.54

[a] $E_{1/2} = (E_{pa} + E_{pc})/2$ where E_{pa} and E_{pc} are the positive and negative peaks potentials, measured on the first scan. [b] $\Delta E_{1/2}$ = difference between first and second reduction potentials. [c] Since polymerization accompanies oxidation of these metalloporphyrins, $E_{1/2}$ values for oxidations are not readily obtained.

chain induces a slight negative potential shift of the $P^{0/\bullet -}$ and $P^{\bullet -/2-}$ couples. A less evident slight shift was observed for the two-electron-oxidation system of the nickel(II) porphyrins, since polymerization accompanies oxidation of these porphyrins. The cyclic voltammograms of the polymerizable complexes (Figure 3B,C) reveal in the positive region one irreversible oxidation peak. The anodic peak i^1_{pa} is abnormally high while its associated cathodic peak i^2_{pc} is low. This behavior is due to the catalytic oxidation of the pyrrole groups by the oxidized forms of the nickel porphyrins[25] since *N*-alkylpyrroles are oxidized around 1.0 V.[10] In addition, Figure 3C shows that this catalytic effect increases with the number of pyrrole-containing groups (R_1) in the monomer, as established by the ratio between i^1_{pa} (anodic peak current for the two-electron porphyrin oxidation) and i^2_{pc} (cathodic peak current for the $P^{0/\bullet -}$ porphyrin system). The ratio of i^1_{pa}/i^2_{pc} increased from 3.1 (**1a** monomer) to 8.7 (**1d** monomer) at a scan rate of 0.1 V s^{-1}.

Electropolymerization and Redox Behavior of the Modified Electrodes. Repeatedly scanning the potential over the

(20) Kadish, K. M. *Phys. Bioinorg. Chem. Ser*. **1986**, *34*, 435.
(21) Nahor, G. S.; Neta, P.; Hambright, P.; Robinson, L. R.; Harriman, A. *J. Phys. Chem.* **1990**, *94*, 6659.
(22) Kadish, K. M.; Franzen, M. M.; Han, B. C.; Araullo-McAdams, C.; Sazou, D. *J. Am. Chem. Soc*. **1991**, *113*, 512.
(23) Bettelheim, A.; White, B. A.; Raybuck, S. A.; Murray, R. W. *Inorg. Chem*. **1987**, *26*, 1009.
(24) Chang, D.; Malinski, T.; Ulman, A.; Kadish, K. M. *Inorg. Chem*. **1984**, *23*, 817.
(25) (a) Deronzier, A.; Latour, J.-M. *J. Electroanal. Chem. Interfacial Electrochem*. **1987**, *224*, 295. (b) Deronzier, A.; Devaux, R.; Limosin, D.; Latour, J.-M. *J. Electroanal. Chem. Interfacial Electrochem.* **1992**, *324*, 325.

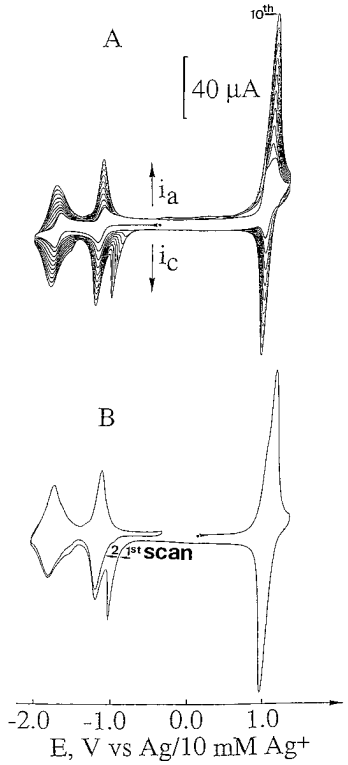

Figure 4. (A) Oxadative electropolymerization of monomer **1a** by repeated potential scans between −2.2 and +1.3 V at a glassy carbon electrode (diameter 5 mm) in CH_3CN + 0.1 M TBAP. Scan rate = 0.1 V s^{-1}. (B) Cyclic voltammogram of a C/poly-**1a** electrode in CH_3CN + 0.1 M TBAP ($\Gamma_{1a} = 8 \times 10^{-9}$ mol cm^{-2}). Scan rate = 0.1 V s^{-1}; scan range −2.1 to +1.3 V.

range from −2.1 to +1.5 V results in a continuous increase in the size of the cyclic voltammetric peaks as shown in Figure 4A. This indicates the formation of an electropolymerized film on the electrode surface as a consequence of the pyrrole oxidation. After a period of scanning (10 cycles, Figure 4A), the glassy carbon electrode covered by a dark blue and adherent thin polymeric film of poly-**1a** was transferred with thorough rinsing to a CH_3CN + 0.1 M TBAP solution free of monomer. The cyclic voltammogram of this modified electrode exhibited the regular electroactivity of the immobilized nickel(II) porphyrin characterized by a reversible two-electron-oxidation wave ($E_{1/2}$ = 1.01 V) and two successive one-electron-reduction waves ($E_{1/2}(P^{0/\bullet -})$ = −1.21 V and $E_{1/2}(P^{\bullet -/2-})$ = −1.76 V) (Figure 4B) as judged by the relative charges under the different peak systems. The regular polypyrrole wave was not observed owing the high positive potential used to elaborate the polymer. As previously described for other functionalized polypyrrole films having no polypyrrole electrochemical feature,[26] the intense prepeak arising at the foot of the first reduction wave disappears on the second scan if the potential scan range is restricted to the negative region (Figure 4B) but is fully restored after a sweep in the positive region up to the oxidation of the macrocycle. This prepeak is a consequence of the resistivity of the film due to the destruction of the regular polypyrrole conductivity.[26] Modified electrodes have also been prepared by controlled-potential oxidation at 0.75 V. For instance, the oxidative electropolymerization of **1d** affords a modified electrode ($\Gamma_{1d} = 5.3 \times 10^{-9}$ mol cm^{-2}) which shows clearly the reversible oxidation of the polypyrrole matrix ($E_{1/2}$ = 0.32 V with an anodic−cathodic peak potential separation (ΔE_p) equal to 0.04 V, υ = 0.1 V s^{-1}) in the positive part of the cyclic

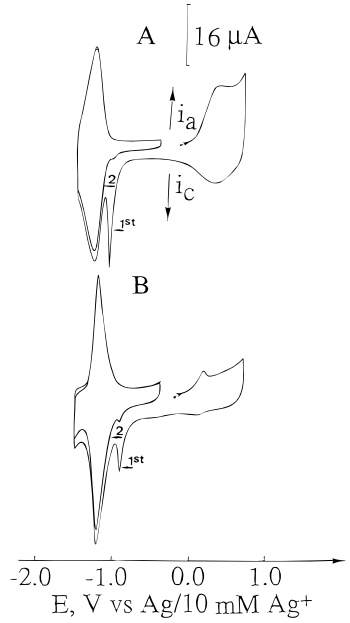

Figure 5. Cyclic voltammograms (A) of a C/poly-**1d** electrode (diameter 5 mm) obtained by oxidative electropolymerization at 0.75 V ($\Gamma_{1d} = 5.0 \times 10^{-9}$ mol cm^{-2}) and (B) of a C/poly-**1a** electrode ($\Gamma_{1a} = 5.0 \times 10^{-9}$ mol cm^{-2}) obtained by a procedure similar to that for (A) in CH_3CN + 0.1 M TBAP. Scan rate = 0.1 V s^{-1}; at controlled potential (E_{app} = 0.75 V).

Table 3. Half-Wave Potentials ($E_{1/2}$) for the C/poly-**1a**−**d** Modified Electrodes in CH_3CN with 0.1 M TBAP (Scan Rate = 0.1 V s^{-1})

	$E_{1/2}$,[a] V (vs Ag/10 mM Ag^+)		
complex	red (2)	red (1)	ox
poly-**1a**	−1.76	−1.21	1.01
poly-**1b**	−1.78	−1.23	1.00
poly-**1c**	−1.80	−1.26	0.98
poly-**1d**	−1.82	−1.28	0.97

[a] $E_{1/2} = (E_{p_a} + E_{p_c})/2$, where E_{p_a} and E_{p_c} are the positive and negative peaks potentials.

voltammogram (Figure 5A). This voltammogram exhibits also a reversible one-electron-peak system ($E_{1/2}$ = −1.28 V, ΔEp = 0.03 V, υ = 0.1 V s^{-1}) corresponding to the $P^{0/\cdot -}$ couple. Figure 5B shows the cyclic voltammogram of the C/poly-**1a** electrode ($\Gamma_{1a} = 5.0 \times 10^{-9}$ mol cm^{-2}), which depicts an electrochemical behavior similar to that of poly-**1d** film. The cyclic voltammetric data for the poly-**1a**–**d** films are summarized in Table 3. It should be noted that the negative region of the cyclic voltammograms (Figures 5A,B) is limited to the first reversible one-electron-peak system but the second reversible one-electron-peak system was also observed likewise in Figure 4B (see Table 3). Although the two modified electrodes contain similar amounts of polymerized nickel(II) porphyrins, the polypyrrole response for poly-**1d** is obviously more markedly evident than that for poly-**1a**. The electropolymerization yields were determined by dividing the charge under the one-electron reduction peak of the nickel porphyrin in the film by the charge passed during the electropolymerization and multiplying by 2.33*n* (*n* being the number of pyrrole groups linked to the macrocycle).[27] It appears that the electropolymerization yield depends strongly on the number of electropolymerizable groups. The best result was obtained with the poly-**1d** film (20%) while the yield for the poly-**1a** film was found to be equal to 8%. In

(26) Cosnier, S.; Deronzier, A.; Roland, J.-F. *J. Electroanal. Chem. Interfacial Electrochem.* **1990**, *280*, 133.

(27) The 2.33 factor used here corresponds to the number of electrons involved in the electropolymerization of the pyrrole (2 electrons molecule^{-1}) plus that for the electrooxidation of the polypyrrole chain (0.33 electron molecule^{-1}).[10]

addition, the electrochemical stability of these poly-**1a** and poly-**1d** modified electrodes was investigated by repeatedly scanning the electrode potential at 0.1 V s^{-1} over the oxidation wave. A slow decrease in the intensity current of the peaks (35% and 20%) was observed after 65 cycles with the poly-**1a** (monosubstituted) and the poly-**1d** (tetrasubstituted) films, respectively. The better redox stability of the poly-**1d** film could be related to a high degree of cross-linking for this polymer due to the presence of four pyrrole-containing groups (R_1) on the macrocycle.

Electroactive Solute Permeation in the Polymeric Films. Since the ferrocene and polypyrrole electrochemical responses are close together, the permeation measurements were performed at polymeric films without the polypyrrole feature to avoid mixing of the two signals. Thus, the destruction of the polypyrrole response by overoxidation was accomplished by repeatedly scanning the potential in range from 0 to 1.5 V.[26] The permeation rate (P_E) is expressed as the ratio of the current peaks for direct oxidations of ferrocene (Fc) or bis(pentamethylcyclopentadienyl)iron (DmFc) at the modified electrodes and at a bare glassy carbon electrode.[28] The permeation measurements were performed in 2 mM solutions of Fc and DmFc in CH_3CN + 0.1 M TBAP. The cyclic voltammograms for permeant Fc at a bare electrode and at a poly-**1a** electrode ($\Gamma_{1a} = 5 \times 10^{-9}$ mol cm^{-2}) show that the current peaks for direct oxidation of Fc are nearly identical in both voltammetric curves ($P_E \approx 1.0$). A similar permeation measurement with this poly-**1a** film was accomplished utilizing DmFc as permeant and the signal was not attenuated ($P_E \approx 1.0$), showing no molecular size discrimination of poly-**1a** film toward either solute in contact with it (molecular sieving property). The same experiment was repeated with the poly-**1d** film exhibiting a similar apparent surface coverage ($\Gamma_{1d} = 5 \times 10^{-9}$ mol cm^{-2}). The response was largely attenuated for permeant Fc ($P_E = 0.22$), and no signal was detected for the bulky DmFc, showing molecular size discrimination of poly-**1d** films in relation to the structure containing one pyrrole-containing group (**1a**), which could lead to construction of a linear chain, and that conformed with four pyrrole-containing groups (**1d**), which could allow a strong cross-linking structure.

Spectroelectrochemistry of the Films. Only results for poly-**1a** are presented here. Poly-**1a** film was grown on an OTE doped with ITO by controlled-potential oxidation at 0.75 V and transferred with thorough rinsing to a pure CH_3CN + 0.1 M TBAP solution. The initial visible spectrum for poly-**1a** film without application of potential, as for the **1a** monomer in solution, presents the expected three absorption bands at 400, 521, and 555 nm. The visible spectrum of the electrooxidation at 1.4 V of a poly-**1a** film on an OTE indicates that the main absorption band of the doubly oxidized form of the film changes from 400 to 334 nm. This behavior could be due to the fact that the oxidation is more likely localized on the metalloporphyrin ring at room temperature.[29] Morever, similar spectral evolution was recently reported by Gray and co-workers[30] for the double-oxidized species of nonplanar zinc(II) tetrakis(pentafluorophenyl)porphyrin in CH_2Cl_2 solution. The spectra of the singly and doubly reduced forms at −1.4 and −1.9 V, respectively, exhibit a significant decrease of the main absorption band at 400 nm. Furthermore, the electroreduction of the poly-**1a** film induces the appearance of broad bands between 600 and 700 nm. This suggests that the one- and two-electron reductions are more likely localized on the immobilized metalloporphyrin rings.[22]

Conclusions

We have synthesized and characterized a new series of nickel(II) *meso*-tetrakis (polyfluorophenyl)porphyrins functionalized by pyrrole-containg groups. It should be noted that this is the first example of polyfluorinated substituted porphyrins where the four possible compounds were obtained by functionalization of the *para*-fluorine substituents of the aryl groups. The electropolymerization of these nickel(II) porphyrins (**1a**−**d**) allows the easy obtention of films exhibiting the regular electroactivity of N-substituted polypyrroles as well as the spectroscopic and electrochemical features of the nickel(II) porphyrins. The investigation of the redox stability and permeability of the metalloporphyrin films has illustrated the influence of the cross-linking degree of the polymeric structure. Application of this kind of electrode material based on other metals like Fe and Mn for biomimetic oxidations and biosensoring is now under investigation.

Acknowledgment. M.A.C.d.M. gratefully acknowledges CAPES (Coordenaçao de Aperfeiçoamento de Pessoal de Nivel Superior)—Foundation of Education—Brazil for a Ph.D. scholarship.

IC9510268

(28) Cosnier, S.; Deronzier, A.; Roland, J.-F. *J. Electroanal. Chem. Interfacial Electrochem.* **1991**, *310*, 71.

(29) (a) Fajer, J.; Borg, D. C.; Forman, A.; Dolphin, D.; Felton, R. H. *J. Am. Chem. Soc.* **1970**, *92*, 3451. (b) Seth, J.; Palaniappan, V.; Bocian, D. F. *Inorg. Chem.* **1995**, *34*, 2201 and references cited therein.

(30) Hodge, J. A.; Hill, M. G.; Gray, H. B. *Inorg. Chem.* **1995**, *34*, 809.